Journal Name

ARTICLE

Photonic vortices induced in single-component phototropic liquid crystal†

Received 00th January 20xx,
Accepted 00th January 20xx

DOI: 10.1039/x0xx00000x

www.rsc.org/

K. Dradrach*, S. Bartkiewicz and A. Miniewicz

Using direct coupling mechanism of light with a liquid via molecular absorption, i.e. opto-thermal effect, we demonstrate the formation of well-controlled three-dimensional circular flows i.e. toroidal vortex, inside the liquid crystal (LC) droplet placed on a glass plate in its isotropic phase. We investigated the behavior of a droplet formed of phototropic liquid crystal and composed of mesogenic azobenzene derivative under the Gaussian beam light illumination in four different geometries. The light-induced liquid flows in isotropic phase of LC were visualized by dispersing carbon micro-particles in the volume of LC. Movements of the particles could be observed under optical microscope from the top and side views, respectively. The direction of stable in time toroidal vortex (the photonic vortex) is dependent on laser light illumination geometry, properties of liquid and substrate but does not depend on gravitational forces being similar for droplets situated either above or below the glass plate. The main mechanism of the indirect conversion of light into mechanical work is related to the temperature induced gradient of surface tension known as Marangoni effect.

A Introduction

Strongly absorbed laser light is rarely used in experiments with liquid samples due to inevitable production of heat transfer and hydrodynamic flows that disturb measurements and are hardly to be controlled. However, at the same time this is the most efficient, though indirect, way to convert light into mechanical work. Harnessing the energy of photons is a far more powerful process than momentum transfer from photons to matter. Direct light momentum transfer or indirect, by coupling optical heating with surface tension gradients have already been used for trapping and actuation of the objects at the nano-, micro- and macro-scale.[1-6] Elegant light controlled movement of objects flowing on water surface has been demonstrated due to strong light absorption of vertically aligned carbon nanotube forests (VANTs) covering those objects.[7] The driving force of the movement was due to heat relaxation introducing gradient of surface tension that draws the liquid flow away from low-surface tension regions. This phenomenon is known as Marangoni effect.[8] Intensive research has been devoted to investigate the behavior of droplets of liquid on various substrates using temperature gradients.[9-12] The recent paper of Pradhan and Panigrahi[13] reports on the study of the fluid flow inside a water droplet placed on a hydrophobic surface subjected to a temperature gradient. Despite the broad treatment of droplet behavior in temperature gradients there is a lack of study of droplets in the temperature gradients caused by direct light absorption of the laser beam.

This work is closely related to the recently published by us paper[14] on observation of light induced whirls in solution of para-nitroaniline in 1,4-dioxane. Solution with para-nitroaniline concentration close to saturation one was deposited on glass plate and illuminated with strongly absorbed laser light beam. As effect of local heating of liquid layer we observed a formation of dense droplet at the illumination spot containing increasing with illumination time concentration of para-nitroaniline. The droplet formation was enhanced by thermocapillary liquid flows from the area surrounding laser beam toward beam center. These liquid flows observed earlier are in certain extent similar to the ones that will be presented in this report except observation of separate droplet formation. The mechanism of the phenomenon reported in [14] due to its complexity is still unknown but its physics is definitely related to Marangoni effect and thermocapillary effects discussed previously in literature, e.g. in [15,16]. In this work we wish to check whether similar effects as in [14] can appear but in quite different system. We decided to use a single component azobenzene based phototropic liquid crystal (PtLC) in its isotropic phase. Absorbed laser light is able to produce cis-isomers from trans-isomers making that the liquid crystal becomes an isotropic liquid.

Advanced Materials Engineering and Modelling Group, Department of Chemistry, Wroclaw University of Technology, Wybrzeze Wyspianskiego 27, 50-370 Wroclaw, Poland. E-mail: klaudia.dradrach@pwr.edu.pl

†Electronic Supplementary Information (ESI) available: Five short video movies described in the text as M1 to M5 accompany this work and complement the descriptions in the text of formation and behavior of photonic vortices. See DOI: 10.1039/x0xx00000x

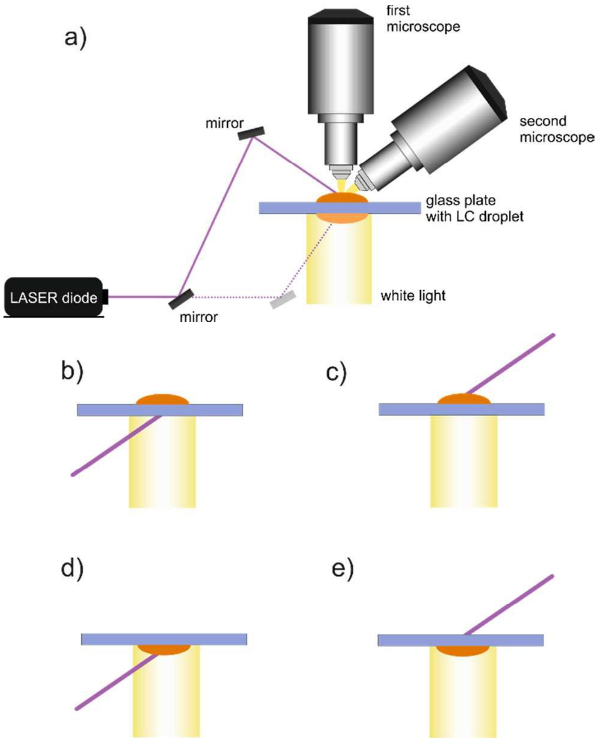

Fig. 1 (a) Scheme of polarizing optical microscope (POM) set-up for observation of laser induced photonic vortices in isotropic phase of PtLC droplets. Various configurations of droplet illumination by Gaussian laser beam of 405 nm wavelength are shown in (b) to (e) figures. In configurations (d) and (e) droplet is upside down.

We decided to use a phototropic liquid crystal in its isotropic phase that absorbs light in the visible part of the spectrum due to presence in mezogenic molecular structure of azo-group undergoing photoisomerisation of *trans* to *cis* type. We study laser induced 3D flow fields inside a liquid crystal droplet illuminated by loosely focused laser beam by microscopic observation of carbon micro-objects following liquid flows. Four different configurations of light illumination carried out in microscope set-up allowed us to draw conclusions about the origin of observed hydrodynamic instabilities.

B Results and discussion

B1 Laser assisted microscopy investigations

The droplet of isotropic liquid is placed on a clean microscope slide (2.5 x 7.5 cm) situated on optical microscope table as shown in Fig. 1a. Typical sizes of investigated droplets were 2 mm in diameter and about 100-200 µm in the thickness at the central part of the droplet. The droplet can be regarded as sessile drop situated on non-wetting substrate, which shape is determined by the contact angle θ_c (here around 20°) that the liquid makes at the three-phase (solid, liquid, gas) contact line, in accordance with the Young–Dupré equation[17]. Under static conditions and assuming interfacial tension γ, the drop shape must also satisfy the Young–Laplace equation of capillarity. We also studied configurations when the droplet was inverted i.e. hanging down below the glass plate. The behavior of liquid could be observed using two microscopes with objectives working in transmission mode. During experiments with laser light the surface of the liquid was monitored from the top and side simultaneously. We have used a CCD camera for registration of droplet behaviors under four different geometries of illumination which are schematically shown in Fig. 1b to 1e. In configuration labelled b) and c) the supported by glass plate droplet is illuminated with the laser beam either from the bottom or top whereas in configurations d) and e) droplet is hanging down kept with capillary forces to the glass plate and also illuminated from its bottom or top. The four configurations were designed in order to establish the main physical effects responsible for the liquid flow inside the droplets heated by laser beam. Laser beam of wavelength λ = 405 nm and a Gaussian shape was used for illumination of the droplets:

$$I(x,y,z) = I_0 \cdot (w_0/w(z))^2 \cdot e^{-\frac{2(x^2+y^2)}{(w(z))^2}}, \qquad (1)$$

where w_0 is beam waist radius and I_0 is the incident laser intensity (here I_0 = 1.8. kW/cm^2, laser power P = 100 mW and the beam crossection area S = 5.4 10^{-3} mm^2). Beam was incident on the droplet either from the bottom (via glass plate) or from the top (directly on liquid-air interface).

B2 Properties of phototropic liquid crystal

As working fluid for the experiment we used the azobenzene

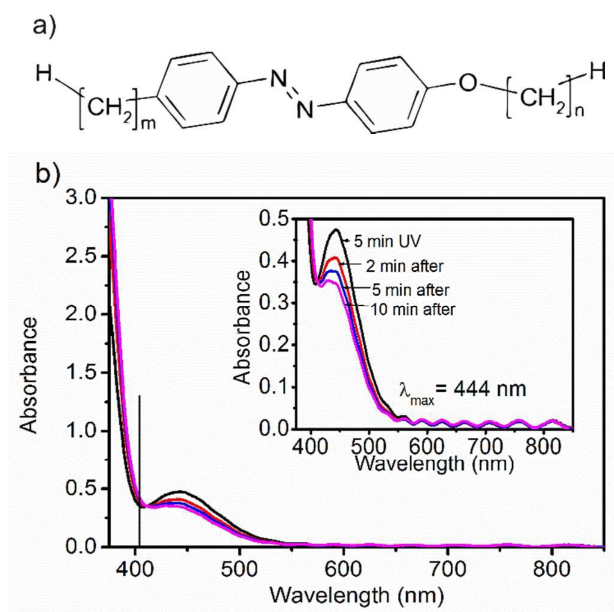

Fig. 2. (a) Molecular structure of 4-alkylo-4'-alkoxyazobenzene mesogenic unit; (b) Photochromism and absorption spectrum of 5-AB-O1 after irradiation with UV light above 67.1°C. Vertical line indicates position of used laser wavelength 405 nm hitting the edge of strong absorption band assigned to *trans* state absorption. UV illumination increases absorption band assigned to *cis* state absorption with maximum at 444 nm.

liquid crystal, 4-alkylo-4'-alkoxyazobenzene. This is a single component phototropic liquid crystal (PtLC). Phototropic liquid crystals form a new class of LCs in which the phase transition from LC to isotropic state is induced by the light. The most exploited phototropic LCs are those based on the azobenzene derivatives, e.g. with general molecular structure m-AB-On shown in Fig. 2a. Particularly we have used 4-pentyl-4'-methoxyazobenzene with m=5 and n=1, abbreviated as: 5-AB-O1. The absorption spectrum of this compound 5-AB-O1 in its isotropic liquid form is shown in Fig. 2b. The 5-AB-O1 is both thermotropic[18] (Cr 40.0ºC N 67.1ºC I) and phototropic LC[19,20]. The reversible photoisomerization of this molecule is accompanied by a significant change in its molecular shape from an elongated rod-like *trans*-form into a bent-core *cis*-form. The *trans*-isomer stabilizes the LC phase whereas the bent *cis*-isomer introduces disorder leading to appearance of isotropic phase. The *trans-cis* isomerization takes place upon exposure to violet light whereas the back reaction *cis-trans* occurs when irradiated by the visible light or due to the thermal *cis*-isomer relaxation. UV light irradiation of crystal 5-AB-O1 at room temperature leads to formation of nematic phase which subsequently, due to released heat, transforms into isotropic liquid. In Fig. 2b we present absorption spectra taken at temperature above 67ºC just after illumination for 5 min by UV lamp light and then after 2, 5 and 10 minutes. Sample for absorption measurements were contained between two glass plates.

Seen in the absorption spectrum (*cf.* inset to Fig. 2b) clear interference above 550 nm allowed us to calculate the sample thickness to be H = 2.85 µm under assumption of average refractive index of isotropic liquid at 800 nm as n_{800} = 1.60. Then absorption coefficient at 405 nm was calculated to amount α_{405} = 2830±50 cm^{-1}. The back thermal reaction *cis-trans* at 67.1ºC occurs relatively fast.

This liquid phase has been treated by us as Newtonian's liquid with strong light absorption at 405 nm and relatively weak evaporation rate under studied conditions. In fact it is not necessary to rise temperature above 67.1ºC to get an isotropic phase. It is sufficient to increase the population of *cis*-isomers (e.g. by using laser light) in the 5-AB-O1 that effectively introduce a disorder leading to appearance of isotropic liquid phase even at room temperature for some time.

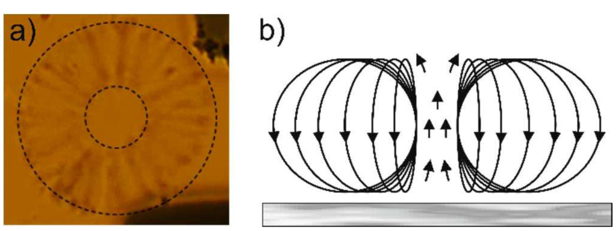

Fig. 3. Top view of carbon microparticles captured during their movement in laser induced toroidal vortex (a), the dashed lines help to determine the region of microparticles movements; (b) schematic side view of tentative circular orbits of microparticles for illumination from the bottom.

B3 Behavior and geometry of photonic vortices in LC isotropic liquid

When a flat layer of liquid PtLC with dispersed in its volume carbon microparticles is illuminated from the bottom (see Fig. 1b) at certain conditions of laser power (P ≈ 100 mW) one observes the concerted movements of microparticles (see movie M1 in Electronic Supplementary Information, ESI). From top view it resembles a projection of a vortex ring (or toroidal vortex) centered on central point where the laser beam hits the liquid (*cf*. Fig. 3, just reflecting at least cylindrical symmetry with axis normal to the glass plate). A toroidal vortex is a donut-shaped region of fluid circulation propelled by axial temperature gradient caused by laser beam absorption and heat release that we call the photonic vortex. Microparticles reflect the flow of liquid inside a layer and are most probably circulating on the stable orbits. The size (diameter) of the whole toroidal vortex based on the photographed carbon microparticles traces is about 500 µm. The inner ring have diameter of 160 µm. The center of this inner ring indicates the position of a laser beam inducing thermal gradients which have diameter of around 50 µm (not visible on the photograph). The width of microparticles traces (torus) is equal to 180 µm. Then, supposing that the stable whirl is formed only when orbits are circular the radius of the orbit is around r ≈ 90 µm and layer thickness slightly exceeds D ≈ 180 µm.

Using fast camera we were able to determine the speed *v* of carbon particles in the photonic vortex. Depending on conditions the particles perform 30 to 100 rotations per second. Assuming that their average velocities in a stable whirl are constant and taking the circular orbit length as 2πr ≈ 565 µm we can obtain linear velocity of carbon particle movement in range u ≈ 17 to 56.5 mm/s. Moving the microscope table, we also move the glass plate with droplet over it and can see a change in position of a toroidal vortex. When laser beam is close to the droplet border the stability of the vortex ceases until its rupture frequently occurring with deposition of the molecular assembly on a substrate. Moving the laser beam again toward the droplet center the stable toroidal vortex is easily recovered (see movie M2 of ESI). However, observations performed under optical microscope of moving carbon particles cannot supply information about the exact direction (upward or downward) of particle movements.

A simple test checking photonic vortex generation was performed by changing the side of illumination of a PtLC layer using the same laser source from the top, i.e. through air-liquid interface (see Fig. 1c). The toroidal vortex was formed as in the previous case but with time the visible traces of deposition of condensed matter (probably carbon particles) on the glass substrate have been observed, suggesting that now the flow is from the top of the layer toward its bottom (see movie M3 of ESI). Deposition of the matter was never observed for illumination from the bottom of the layer, i.e. through glass-liquid interface, suggesting that in this case the particle movement could be from the bottom to the top. This is an interesting finding, as it tells us that the buoyancy effect

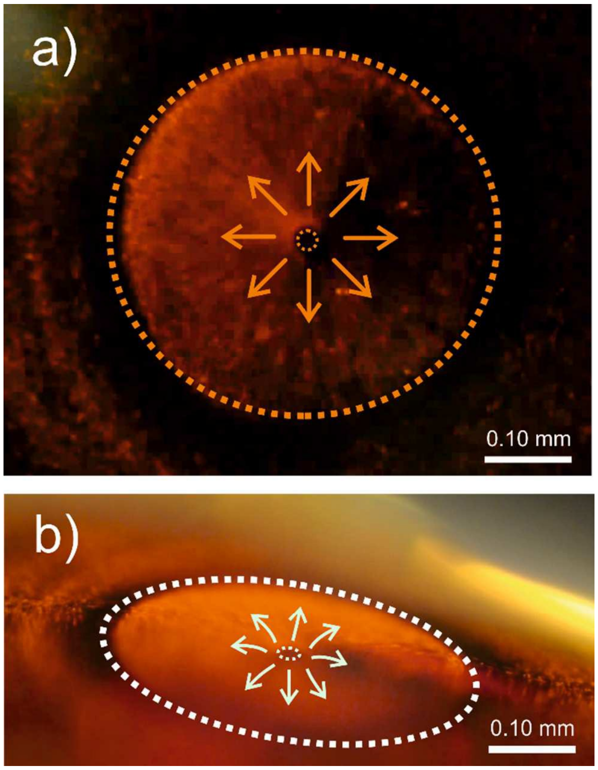

Fig. 4. Top view (a) and side view (b) of a droplet with dispersed carbon particles. When droplet is illuminated from the bottom (through supporting glass) a visible diminishing of absorbance is observed in the droplet center (a); the considerable depression on the surface of the film is seen in side view (b). Large dashed-line circle marks a boundary of photonic vortex. Whereas small dashed-line circle marks a center of vortex and thus the region in which laser beam hits the glass plate. For more clear view see the movie M3 of ESI.

is not a decisive one in determination of liquid flows or particles swirling direction. Supplementary investigations were also performed in inverted geometry i.e. when droplet of PtLC was hanging down. In this case (see Fig. 1d and 1e) there were no signs of matter deposition when illumination was from the top (i.e. from the glass side) and was observed for illumination from the bottom i.e. from the air side. However, we would like to stress that, so far we have no direct evidence of swirl movement direction in the both above discussed cases and that will be checked in the future using a fast camera.

Convincing information about swirling direction is supplied by the second microscope able to monitor the surface of the droplet during laser illumination (*cf*. Fig. 4 and movie M4 of ESI).

The visible depression of the liquid surface in the central part is clearly connected with toroidal vortex formation. The stronger the intensity of laser, the bigger depression of the film is observed. Then apparently the particle orbits can have higher radiuses because around the toroidal vortex center the liquid level increases. Measurements show that a diameter of the torus D is almost linearly dependent on the laser light power P, i.e. in the range of powers from 25 to 50 mW, the slope dD/dP is equal to 12 µm/mW. As expected no dependence of toroidal vortex generation on laser light polarization was observed what confirms the absorption induced effects.

Laser illumination from the top of the liquid layer also leads to surface depression. Having two cameras we performed detailed observation of sample behavior in this case and photographed how the carbon microparticles flowing on the surface of the liquid are drag into the depression region and "feed" the toroidal vortex. This may happen only if their masses are adapted to the swirling speed or are ejected outside the vortex if their masses are too large to be included in the fast fluid movement (see movie M4 and M5 of ESI).

B4 Physics of photonic vortex formation

The conditions of stable toroidal photonic vortex creation require a delicate balance of used beam intensity and its wavelength with properties of investigated liquid, i.e. layer (droplet) height H, liquid layer absorbance α, temperature T, density $\rho(T)$, surface tension $\sigma(T)$, dynamic viscosity $\eta(T)$, specific heat $c(T)$ and heat conductivity $\kappa(T)$. The surface-tension-driven phenomena were exhaustively treated in work of Levich and Krylow[21] and this is not the aim of this work to propose the exact mathematical model to the observed phenomenon. However, we can discuss principal phenomena that are involved in observed photonic toroidal vortex formation. In Fig. 5 we schematically show the mechanism of toroidal vortex formation that constitutes of: (i) the Gaussian laser beam light absorption by the liquid and relevant to it formation of vertical and radial gradient field of temperature, (ii) vertical heat and mass transfer induced by free and Marangoni convection due to gradient of surface tension, (iii) inducement of the toroidal vortex due to fluid flow continuity law directed from the periphery toward the center of the heated zone.

Similar system has been considered earlier by Louchev et al.[22] Laser beam absorption is a source of the heat, then the radial shape and intensity of the beam defines the initial

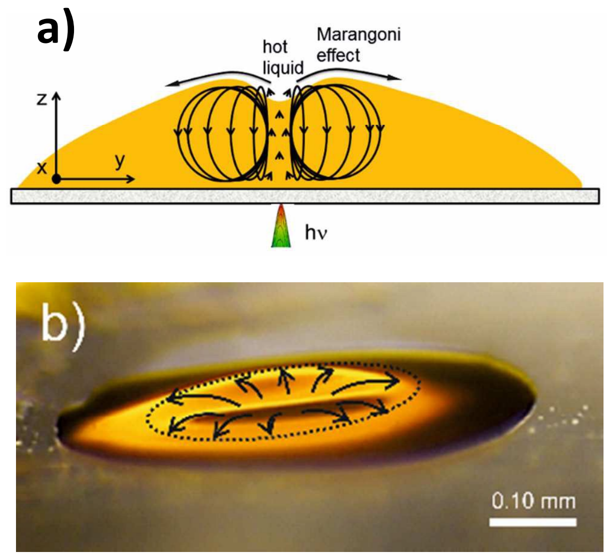

Fig. 5. Schematic view of photonic vortex formation in absorbing liquid (a) the side view of a droplet during laser illumination from the bottom (b).

temperature distribution according to the equation of heat conductance. This process starts convection of a fluid limited by the layer thickness. When a flow reaches the threshold velocity u_{th} the formation of stable mass flux ρ**u** in form of closed loops, i.e. photonic toroidal vortex is observed. The velocity distribution of a fluid element inside droplet is defined through equation:

$$\frac{d\mathbf{u}}{dt} = -\nabla p + \nu\nabla^2\mathbf{u} + \frac{\mathbf{F}}{\boldsymbol{\rho}} \quad (2)$$

which is coupled with the continuity equation $\nabla \cdot \mathbf{u} = 0$, where **u** is the velocity vector, *p* is the pressure, ρ is the density, ν = η/ρ is the kinematic viscosity and **F** is the external force per volume unit. All parameters are dependent on space and time. We can estimate the expected Reynolds (*Re*) and Prandtl (*Pr*) numbers for the typical liquid crystal as 4-pentyl-4´-cyanobiphenyl (5CB) and assume that these numbers are also characteristic for the studied liquid crystal. The Reynolds number *Re* = ρ·*u*·*l*/η , can be calculated using values ρ = 9600 kg/m^3 [23], *u* = 0.0565 m/s (this work), *l* = 200x10-6 m (this work) and η = 0.0245 Pa·s [24] giving *Re* = 4.4. The Prandtl number *Pr* = c_p·η/κ, can be calculated inserting c_p = 1.8 J/g·K [25], thermal conductivity κ = 1.5 mW/cm·K and η = 0.0245 Pa·s [24] as *Pr* = 292. Then our system is described by a small Reynolds (*Re*) number and much larger than 1 Prandtl number (*Pr*), which tells us that the fluid flow is not turbulent and heat dissipation is dominated by mass convection. Non-uniformity of laser-induced temperature causes the fluid motion via two effects: buoyancy and temperature dependent surface tension. The volumetric buoyant force can be approximated by:

$$\mathbf{F} = -\rho\beta\boldsymbol{g}(T - T_0) \quad (3)$$

where β stands for volumetric temperature expansion coefficient $\beta = -\rho^{-1}\frac{\partial\rho}{\partial T}$ and **g** is the gravitational constant vector and *T* is the temperature. The surface tension force comes from the gradient of the temperature at the surface resulting in the shear stress along the surface:

$$\tau = \frac{d\sigma}{dr} = \frac{\partial\sigma}{\partial T}\frac{dT}{dr} = \sigma_T\frac{dT}{dr} \quad (4)$$

that causes the flux of fluid in the direction normal to the surface $\tau = -\nu\rho\frac{du_r}{dz}$ where σ is the surface tension obeying the general boundary condition:

$$\rho\nu\mathbf{n}\nabla\mathbf{u} = \sigma_T\nabla_{||}T \quad (5)$$

In equation (4) **n** is unitary vector normal to the surface and $\nabla_{||}$ is the tangential derivative operator. The surface tension in 5CB is equal to 32 mN/m [27]. As pointed by Louchev et al.[22] for the different physical system the convection develops much faster than the Marangoni effect but the latter can produce very strong enhancement of mass transfer leading finally to appearance of toroidal vortex. The simulation of toroidal vortex is only possible via numerical solution of presented above equations providing the detailed physicochemical parameters of used liquid crystal in its isotropic liquid phase are known. Currently for this compound these physicochemical parameters are not available. However, the complexity of the problem requires simultaneous solution of the equation of heat and mass transfer as well as the hydrodynamic ones.

Conclusions

We have presented laser-light induced photonic toroidal vortex formation in azobenzene derivative liquid crystal compound in its isotropic phase. The observations of fluid flows were made by doping the liquid with carbon particles and using two microscopes vertical and tilted giving the top and side views of the vortex simultaneously. We have checked four different geometries of illumination in order to characterize the mechanism of photonic vortex formation in droplets. We are convinced that the main contribution to the laser induced photonic vortex formation is due to Marangoni effect and not buoyancy one. We anticipate extension of this technique to variety of absorbing liquids in order to get complex information about physicochemical parameters of liquids that enable occurrence of this unique effect. The current as well as the previous demonstration[14] of generation of stable and strong photonic vortices in layers of liquids with their easy movements over the whole liquid area point to the obvious application of laser induced mixing of liquids. Moreover, from our results reported in patent application[28] it follows that the method can be used for transport of microobjects in liquid from one place to another. It is also possible to use this method to help dissolving crystals, to crush agglomerates of nanoparticles, etc. (unpublished yet). From technological point of view very interesting application of photonic vortices could be a matter deposition at the substrate surface including targeted crystal growth.

Acknowledgements

This work was financially supported by the National Science Centre, Poland 2014/15/B/ST8/00115.

References

1 A. Ashkin, *Physical Review Letters*, 1970, **24**, 156.
2 M. E. J. Friese, T.A. Nieminen, N. R. Heckenberg and H. Rubinsztein-Dunlop, *Nature*, 1998, **394**, 348.
3 H. R. Jiang, N. Yoshinaga and M. Sano, *Physical Review Letters*, 2010, **105**, 268302.
4 C. Maggi, F. Saglimbeni, M. Dipalo, F. De Angelis and R. Di Leonardo, *Nature Communications*, 2015, **6**, 7855.
5 D. E. Lucchetta, F. Simoni, L. Nucara and R. Castagna, *AIP Advances*, 2015, 5, 077147.
6 H. Zeng, P. Wasylczyk, C. Parmeggiani, D. Martella, M. Burresi, and D. S. Wiersma, *Advanced Materials*, 2015, **27**, 3883.
7 D. Okawa, S. J. Pastine, A. Zettl, and J. M. J. Frèchet, *Journal of the American Chemical Society*, 2009, **131**, 5396.
8 C. Marangoni, *Il Nuovo Cimento Series 2*, 1872, **5/6**, 239.

9 V. Pratap, N. Moumen and R. S. Subramanian, *Langmuir*, 2008, **24**, 5185.
10 S. Mettu and M. K. Chaudhury, *Langmuir*, 2008, **24,** 10833.
11 H-B. Nguyen and J.-C. Chen, *Physics of Fluids*, 2010, **22,** 062102.
12 Y. Zhao, F. Liu and C.-H. Chen, *Applied Physics Letters*, 2011, **99**, 104101.
13 T. K. Pradhan and P. K. Panigrahi, *Experiments in Fluids,* 2015, **56**, 178.
14 S. Bartkiewicz and A. Miniewicz, Physical Chemistry Chemical Physics, 2015, **17**, 1077.
15 E. Lim and Y. M. Hung, *International Communications in Heat and Mass Transfer*, 2015, **66**, 203.
16 J.-J. Yu, Y.-R. Li, C.-M. Wu and J.-C. Chen, *International Journal of Heat and Mass Transfer*, 2015, **90**, 1071.
17 M. E. Schrader, *Langmuir*, 1995, **11**, 3585.
18 J. Zienkiewicz, *Liquid crystalline properties of 4-alkyl-4-alkyloxyazobenzenes*, 2000, PhD thesis, Wroclaw University, Wroclaw, Poland.
19 A. Sobolewska, J. Zawada, S. Bartkiewicz and Z. Galewski, *Journal of Physical Chemistry C,* 2013, **117**, 27067.
20 A. Sobolewska, S. Bartkiewicz, J. Mysliwiec and K. D. Singer, *Journal of Material Chemistry C*, 2014, **2**, 1409.
21 V. G. Levich and V. S. Krylov, *Annual Review of Fluid Mechanics*, 1969, **1**, 293.
22 O. A. Louchev, S. Juodkazis, N. Murazawa, S. Wada and H. Misawa, *Optics Express*, 2008, **16**, 5675.
23 J. Deschamps, J. P. M. Trusler and G. Jackson, *Journal of Physical Chemistry B*, 2008, **112**, 3918.
24 A. Böttger, D. Frankel, E. van de Riet and R. Zijlstra, *Liquid Crystals*, 1987, **2**, 539.
25 J. Thoen, "Calorimetric Studies of Liquid Crystal Phase Transitions: Steady State Adiabatic Techniques", in: *Phase Transitions in Liquid Crystals*, edited by S. Martellucci and A.N. Chester, Plenum Press, New York, 1992, pp.155-274.
26 G. Ahlers, D. S. Cannell, L. I. Berge and S. Sakurai, *Physical Review E*, 1994, **49**, 545.
27 B. Song and J. Springer, *Molecular Crystals and Liquid Crystals Science and Technology. Section A. Molecular Crystals and Liquid Crystals*, 1997, **307**, 69.
28 S. Bartkiewicz, A. M. Sobolewska, K. Dradrach, „Sposób mieszania i przemieszczania cząstek w materiale ciekłokrystalicznym (Method for mixing and relocating of particles in the liquid crystalline material)", patent application number: P 408349, 2014.

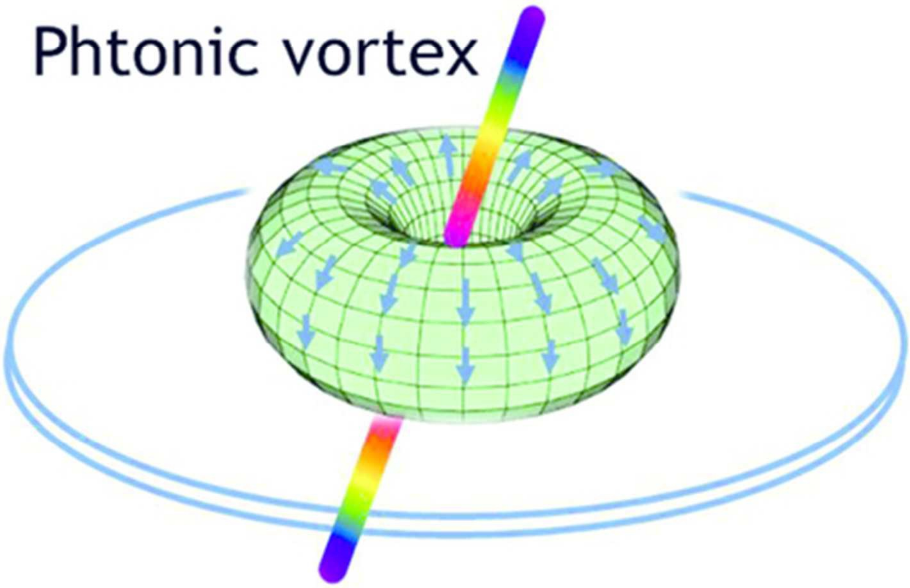

39x29mm (300 x 300 DPI)